View metadata, citation and similar papers at core.ac.uk
brought to you by CORE
provided by Springer - Publisher Connector

DE GRUYTER OPEN

Acta Geophysica
vol. 64, no. 1, Feb. 2016, pp. 237-252
DOI: 10.1515/acgeo-2015-0065

Local Ionospheric Modeling Using the Localized Global Ionospheric Map and Terrestrial GPS

Mohammad Ali SHARIFI[1,2] and Saeed FARZANEH[1]

[1]School of Surveying and Geospatial Engineering,
College of Engineering, University of Tehran, Tehran, Iran;
e-mails: Sharifi@ut.ac.ir, Farzaneh@ut.ac.ir (corresponding author)

[2]Research Institute of Geoinformation Technology (RIGT),
College of Engineering, University of Tehran, Tehran, Iran

Abstract

Global ionosphere maps are generated on a daily basis at CODE using data from about 200 GPS/GLONASS sites of the IGS and other institutions. The vertical total electron content is modeled in a solar-geomagnetic reference frame using a spherical harmonics expansion up to degree and order 15. The spherical Slepian basis is a set of bandlimited functions which have the majority of their energy concentrated by optimization inside an arbitrarily defined region, yet remain orthogonal within the spatial region of interest. Hence, they are suitable for decomposing the spherical harmonic models into the portions that have significant strength only in the selected areas. In this study, the converted spherical harmonics to the Slepian bases were updated by the terrestrial GPS observations by use of the least-squares estimation with weighted parameters for local ionospheric modeling. Validations show that the approach adopted in this study is highly capable of yielding reliable results.

Key words: spherical Slepian functions, spherical harmonics, ionospheric modelling.

Ownership: Institute of Geophysics, Polish Academy of Sciences;
© 2015 Sharifi and Farzaneh. This is an open access article distributed under the Creative Commons Attribution-NonCommercial-NoDerivs license, http://creativecommons.org/licenses/by-nc-nd/3.0/.

1. INTRODUCTION

A layer of atmosphere between the altitudes of about 60 to 2000 km above the Earth's surface is called ionosphere, where the solar radiation produces partially ionized plasma of different gas components. Knowledge about ionospheric electron density and its variation is essential for a wide range of applications. As a result, the ionospheric modeling has received specific attentions in numerous fields of research, including radio communications, navigations, satellite positioning, and other space technologies.

Ionospheric models are divided into three main categories: one group includes physical models, in which ionospheric changes are simulated based on the physical laws or the assumptions concerning the structure and variations of the ionosphere, *e.g.*, the Global Assimilative Ionospheric Model (GAIM) (Schunk *et al*. 2004); another group is known as empirical models, including the International Reference Ionosphere (IRI; Bilitza *et al*. 2011) or the NeQuick (Angrisano *et al*. 2013, Radicella *et al*. 2008); and finally the third group consists of mathematical models, which are mainly based on the observations of the ionosphere.

In the last category, mainly two approaches are applied to model the spatial distribution of ionospheric density using GPS observations, *i.e.*, two-dimensional (2-D) or three-dimensional (3-D) models of the electron density. The 3-D modeling is based on latitude, longitude, and height, in which the slant total electron content (STEC; *i.e.*, the number of electrons which are present in a column of 1 m^2 cross-section and extend along the ray-path of the signal between global positioning system (GPS) satellites and the ground receiver) measurements are inverted into electron density distribution using tomographic approaches (for a comprehensive overview about various techniques of ionospheric density modeling, see, *e.g.*, García-Fernández 2004). As the distribution of permanent GPS reference stations is not globally uniform and does not supply high vertical resolution for ionospheric tomography (García-Fernández *et al*. 2003), additional observations derived from ionosondes, satellite altimetry or GPS receivers on Low-Earth-Orbiting (LEO) satellites have been considered in several 3-D studies (Stolle *et al*. 2003, Schmidt *et al*. 2008, Zeilhofer 2008). Due to the fact that the spatial and temporal distribution of additional observation are usually limited, they can be only applied where or when the observations are available. Therefore, the majority of the GPS-based studies, as the present study, headed towards 2-D modeling, which are fairly well addressed in Wielgosz *et al*. (2003), Mautz *et al*. (2005), and Liu *et al*. (2008). In 2-D approaches, a single-layer model (SLM) tends to be adopted for ionospheric density changes. In this approach, therefore, it is assumed that all free electrons within ionosphere are concentrated in an extremely thin layer at a constant height. Consequent-

ly, the vertical gradient of electron density changes is ignored (Schaer 1999). From this aspect, the vertical profiles of total electron content (VTEC) should be taken into consideration. Since GPS basically provides the measurements of slant total electron content, an elevation-dependent mapping function is required to describe the ratio between the STEC and VTEC.

The single-layer models can fall into two categories of the non-grid- and grid-based maps (El-Arini *et al*. 1994b). The former is based on fitting a set of arbitrary base functions, using the least-squares method, to the total electron content (TEC) observations. The chosen base functions can be polynomial functions as in Coster *et al*. (1992) and Komjathy (1997); spherical harmonics (often upto degree and order 15) as in Schaer (1999); trigonometric functions (Alizadeh *et al*. 2011); the B-Spline functions, which are based on Euclidean quadratic B-Spline wavelets (Schmidt 2007, Schmidt *et al*. 2008, Zeilhofer 2008, Nohutcu *et al*. 2010); adjusted spherical harmonic function model (Schaer 1999); and the spherical cap harmonic functions as in Liu *et al*. (2010, 2011, 2014). The latter is applied to model the ionospheric vertical delays at fixed ionospheric grid points (El-Arini *et al*. 1993, 1994a; Gao *et al*. 1994, Skone 1998, Liao and Gao 2001).

A common way of VTEC modeling is based upon the spherical harmonic expansions, whose efficiency requires an availability of the regularly distributed global data. On the other hand, to explain high frequency ionospheric variations, one requires to increase the degree and order of the spherical harmonics. This, in fact, decreases the computational efficiency, particularly for the real-time applications due to the computational load. The bias introduced through the data cut-off at the boundaries (the Gibbs phenomenon) is another drawback to the regional modeling of the ionosphere using global spherical harmonic base functions (Mautz *et al*. 2005, Schmidt 2007). In other words, although modeling based on the spherical harmonics is a well-understood and convenient apparatus for the global representation and analysis of the ionosphere, it lacks the flexibility to identify the spatial and spectral structure of such fields from the "spatiospectrally" mixed vantage point (Beggan *et al*. 2013).

The so-called spatiospectral concentration problem can be solved by determining an orthogonal family of the strictly bandlimited functions that are optimally concentrated within a closed region of the sphere, or by considering an appropriate orthogonal family of the strictly spacelimited functions that are optimally concentrated in the spectral domain (Simons *et al*. 2006). One attempt to improve the spatial selectivity of spherical-harmonic-based representations was applied based on the wavelet analysis (Simons *et al*. 1997). In this approach, some selected windows, corresponding to particular spectral degree ranges, are applied via convolutions to conduct a space-spectral analysis approach (Schmidt 2007). The drawback of methods based

on wavelet analysis was that the area of the spatial (target) region scales inversely with the degree of base functions (Beggan *et al*. 2013). In other words, base functions cannot be bandlimited and spacelimited at the same time. This can be exemplified by considering a spatial (binary) mask over a region of interest as: by definition, the mask is perfectly localized in the space domain, but it represents an almost infinite dimensional ringing behaviour in the spectral domain. Representing the mask by bandlimited wavelets would thus yield undesirable spectral-domain artefacts. Therefore, tapering or boxcar techniques are usually used to lose some spatial selectivity to improve spectral representation (Tegmark 1997, Beggan *et al*. 2013).

As an optimum trade-off between bandlimited and spacelimited representation, one can use the Slepian basis that can be applied as windows for spectral analysis, or as a sparse basis to represent and analyze geophysical observables on a sphere (Wieczorek and Simons 2005, Simons *et al*. 2006). Such a trade off between spectral and spatial concentrations on the surface of a unit-radius sphere is optimized by constructing a particular linear combination of spherical harmonics (Simons *et al*. 2006). As a result, the global signals can be decomposed effectively into the selected regional base functions, which optimally approximate the regional field and localize it over an area of interest. Thereby, the corresponding spherical-harmonic spectrum can be studied robustly.

As compared to other regional ionospheric modeling techniques, most of the aforementioned techniques do not contribute to the optimization of the field separation over regions with irregular boundaries. For instance, the spherical cap technique provides a great opportunity by reducing the lack of orthogonality of the global spherical harmonic over local regions. The method, however, requires a symmetric boundary definition when performing the fitting procedure. In contrast, we propose the use of the Slepian functions to model ionospheric changes in regions with irregular boundary shapes. This characteristic is important to assess the spectral characteristics of regions with distinct geographical property with less (spectral) contribution from the neighboring regions.

In this study, the converted spherical harmonics to the Slepian base functions was combined with the terrestrial GPS observations, using a least-squares estimation with weighted parameters, in order to estimate local ionospheric maps.

2. TEC DETERMINATION

In this study, a method of measuring TEC directly from the differential code delay and carrier phase measurement on both the L1 and L2 frequencies was used. For this purpose, the carrier to code leveling process method (Ciraolo

et al. 2007, Nohutcu *et al*. 2010) was used. The necessary formula can be extracted from Gao *et al*. (1994), Liu *et al*. (2011), and Wu *et al*. (2010).

2.1 Global ionospheric model of the CODE

The center for orbit determination in Europe (CODE) is one of the international global navigation satellite system (GNSS) service (IGS) analysis centers which determine the precise GPS orbit by using IGS network observation data and provide the orbit information for the worldwide GPS users. The CODE has also produced the daily maps of the Earth's ionosphere on a regular basis since 1 January 1996. The global ionosphere map (GIM)/CODE is modeled with 256 coefficients of SH expansion up to 15 degrees and 15 orders. Thirteen GIMS and their errors at 2-hour intervals are included in a GIM/CODE data, which is accessible at ftp://ftp.unibe.ch/aiub/CODE/. The principles of the TEC mapping technique used at CODE were described in Schaer *et al*. (1995, 1996).

3. SPHERICAL SLEPIAN FUNCTIONS

Given that (i) the time-variable TEC signals are located in specific regions of interest; and that (ii) the TEC data is discretely measured by the ground-based GPS observations and, therefore, has a band limit; and that (iii) some portion of the spectrum where the error terms are expected to dominate is excluded as desired, then an orthogonal basis on the sphere, which is both optimally concentrated in our spatial region of interest and bandlimited to a chosen degree, would be expected. For this purpose, the Slepian function was used for regional ionospheric modeling.

An arbitrary real-valued, square-integrable function $f(\vec{r})$ on the unit sphere can be expressed by spherical harmonic expansions as:

$$f(\vec{r}) = \sum_{l=0}^{\infty} \sum_{m=-l}^{l} f_{lm} Y_{lm} \ , \tag{1}$$

where f_{lm} is the spherical harmonic coefficient:

$$f_{lm} = \frac{1}{4\pi} \int_{\Omega} f Y_{lm} d\Omega \ . \tag{2}$$

$Y_{lm}(r)$ is the real spherical harmonics of degree l and order m, which is defined for each point r on a unit sphere Ω with colatitude θ and longitude λ as:

$$Y_{lm}(r) = Y_{lm}(\theta, \lambda) = \begin{cases} \sqrt{2} X_{l|m|}(\theta) \cos m\lambda & \text{if} \quad -l \le m < 0 \ , \\ X_{l0}(\theta) & \text{if} \quad m = 0 \ , \\ \sqrt{2} X_{lm}(\theta) \sin m\lambda & \text{if} \quad 0 \le m < l \ , \end{cases} \tag{3}$$

where

$$X_{lm}(\theta) = (-1)^m \left(\frac{2l+1}{4\pi}\right)^{1/2} \left[\frac{(l-m)!}{(l+m)!}\right]^{1/2} P_{lm}(\cos\theta) \quad . \tag{4}$$

and $P_{lm}(\mu)$ is an associated Legendre polynomial. These spherical functions form a set of the orthonormal bases for the square-integrable and real-valued functions on the unit sphere. It is noteworthy that the spherical harmonics have a global support. Therefore, they are not suitable for the local data modeling. Here, we are interested in the space of the square-integrable functions with no power above the bandwidth L. That is, f belongs to the space of bandlimited functions denoted by:

$$B_L = \left\{ f \in L^2(S) \middle| f = \sum_{l=0}^{L} \sum_{m=-l}^{l} f_{lm} Y_{lm} \right\} . \tag{5}$$

Simons *et al*. (2006) solved the problem of concentrating a real-valued function simultaneously in the spatial and the spectral domain, leading to the so-called Slepian functions. In order to localize spherical harmonic functions into a region of interest R (the target region), the optimization of a local energy criterion (Eq. 8) can be utilized. This will give a new set of functions in the sense of Slepian (1983). They are bandlimited to the maximum spherical harmonic degree L and, at the same time, are spatially concentrated inside the target region. In other words, the Slepian basis set is merely a unitary linear transformation of the spherical-harmonic basis, but it is the spatial region of interest, built into their construction via quadratic maximization, that leads to their efficiency for the modeling of the regional signals (Beggan *et al*. 2013). The spherical Slepian function can be presented as a bandlimited spherical harmonic expansion:

$$g(r) = L \sum_{l=0}^{\infty} \sum_{m=-l}^{l} g_{lm} Y_{lm}(r) \tag{6}$$

with

$$g_{lm} = \int_{\Omega} g(r)\, Y_{lm}(r) d\Omega \tag{7}$$

which is obtained by maximizing the energy concentration:

$$\lambda = \max \frac{\int_R g^2 d\Omega}{\int_{G^\Omega} g^2 d\Omega} \quad , \tag{8}$$

where $0 \le \lambda \le 1$ is a measure of the spatial concentration. By substituting Eq. 6 into Eq. 8, we get:

$$\lambda = \frac{\sum_{l=0}^{L}\sum_{m=-l}^{l} g_{lm} \sum_{l'=0}^{L}\sum_{m'=-l'}^{l'} D_{lm,l'm'} g_{l'm'}}{\sum_{l=0}^{L}\sum_{m=-l}^{l} g_{lm}^2} \tag{9}$$

where

$$\mathrm{D}_{lm,l'm'} = \int_R Y_{lm} Y_{l'm'} d\Omega \ . \tag{10}$$

The elements of $(L+1)^2 \times (L+1)^2$ localizing kernel D can be introduced as:

$$D = \begin{pmatrix} D_{00,00} & \cdots & D_{00,LL} \\ \cdot & & \cdot \\ \cdot & & \cdot \\ D_{LL,00} & \cdots & D_{LL,LL} \end{pmatrix} \tag{11}$$

and g is the $(L+1)^2$ dimensional vector, which represents a Slepian eigenfunction expressed in the spherical harmonics:

$$g = \left(g_{00} \cdots g_{lm} \cdots g_{LL} \right)^T \tag{12}$$

which is associated with the function $g(\vec{r})$ and is orthogonal over the whole sphere Ω and over the region R. Equation 8 can be written as a classical matrix variational problem as:

$$\lambda = \frac{g^T D g}{g^T g} \to \max \ . \tag{13}$$

The maximization of this concentration criterion can be achieved in the spectral domain by solving the algebraic eigenvalue problem (Simons *et al.* 2006):

$$Dg = \lambda g \ . \tag{14}$$

The matrix D is real, symmetric, and positive definite (Simons *et al.* 2006) so that the $(L+1)^2$ eigenvalues λ and the associated eigenvectors g are always real (Horn and Johnson 1991).

When the signal $g(r)$ is local, it can be approximated using the Slepian expansion truncated at the Shannon number N (Percival and Walden 1993):

$$N = \sum_{n=1}^{(L+1)^2} \lambda_n = (L+1)^2 \frac{A}{4\pi} \ , \tag{15}$$

where A is the area of the region as a fraction of the whole sphere. The data can be approximated, yet with very good reconstruction properties within the region by (Simons 2010):

$$d(\hat{r}) \approx L\sum_{n=1}^{\dot{N}} d_n g_n(\hat{r}) \ , \tag{16}$$

where $g_n(\hat{r})$ and d_n are the spherical Slepian function and unknown coefficient, respectively.

3.1 Converting spherical-harmonic coefficients into Slepian coefficients

As already said, spherical surface harmonics are functions of global support that can be converted, by a unitary linear transformation, into a spherical Slepian basis whose energy is concentrated onto specific patches of the sphere (Wieczorek and Simons 2005, Simons *et al*. 2006, Beggan *et al*. 2013). The goal of this section is to convert spherical surface harmonics which are functions of the global support into a spherical Slepian basis whose energy is concentrated onto the specific patches of the sphere by a unitary linear transformation. The known harmonic field $V(\theta,\lambda)$ can be localized inside a default region by:

$$V^{\text{localized}}\left(\theta,\lambda\right) = \left(gg^T\right) f \ , \tag{17}$$

where f is a spherical harmonic coefficient (in this case, the CODE global ionospheric model), g is a localization matrix (Eq. 7). Figure 1 illustrates the steps for this procedure schematically.

4. COMBINING SLEPIAN COEFFICIENTS BY THE TERRESTRIAL GPS OBSERVATIONS

After converting spherical harmonics to Slepian coefficients, they were combined with the Slepian coefficients obtained by the terrestrial GPS observations with the help of the least-squares adjustment with weighted parameters, as discussed in detail by Mikhail and Ackermann (1976). The normal equation can be obtained by:

$$\left(A^T P_l A + H^T P_x H\right) X = \left(A^T P_l l + H^T P_x l_x\right) \ , \tag{18}$$

where A is the $n \times u$ coefficient matrix with full column rank; n is the total number of observations; u is the number of unknowns; that is, the total number of unknown Slepian coefficients collected in the $u \times 1$ vector X; P_l is the known positive definite $n \times n$ weight matrix of the observations collected in the $n \times 1$ vector l; H is the identity matrix and l_x contains *a priori* Slepian coefficients value (the converted spherical harmonics coefficients) with weight matrix P_x.

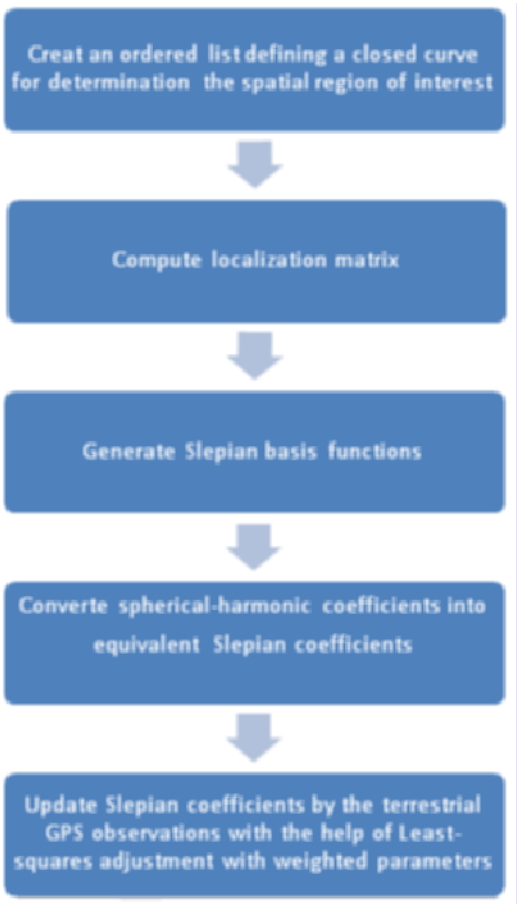

Fig. 1. Procedure for combine Slepian coefficients by the terrestrial GPS observations.

5. RESULTS AND DISCUSSION

The regional VTEC modeling in this study is based on the ground-based GPS observations collected across the western part of the United States of America (USA). The 24 h observations of 30 stations belong to IGS networks, are obtained through the internet, and the sampling rate of the measurements is 30 s. The distribution of the stations has been illustrated in Fig. 2. In order to solve STEC from observations, the receiver inter-frequency biases (IFBs) were calculated using the Bernese GPS software v5.0 and the IFB values for the satellite were obtained from the CODE. The STEC and VTEC values for each observation were computed as described in Section 1. The altitude for the single layer model was set to 400 km for the

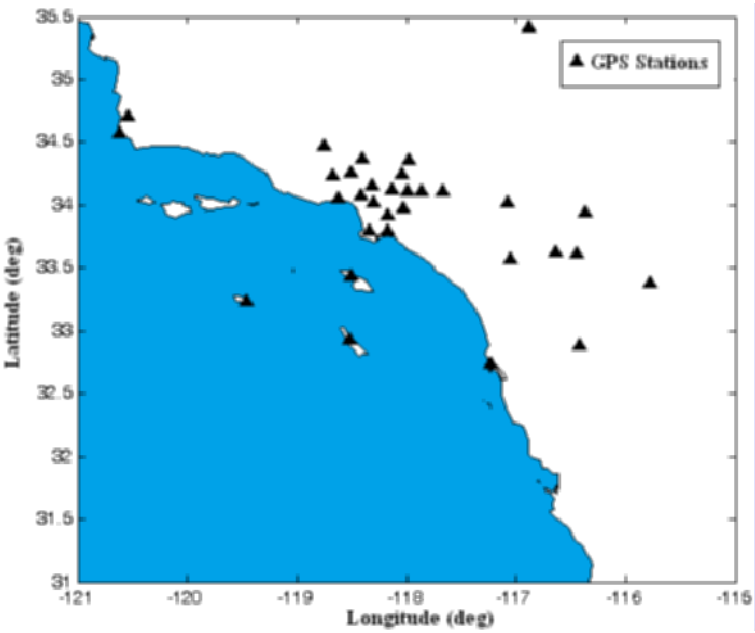

Fig. 2. Distribution of GPS reference stations.

calculation of VTEC and the elevation cut-off angle of 15° was used. The precise orbit files, provided by several IGS agencies, were interpolated to determine satellite positions. These TEC measurements contain the ionospheric electron density information about region above the GPS network and are used as the input data for the ionospheric modeling. The spherical harmonic coefficients from Global Ionospheric Maps provided by the CODE, an analysis center within the IGS, were used for the localization approach. The data contains a full set of coefficients to degree and order 15 (*i.e.*, $n_{\max} = 15$) and represents the ionosphere as an infinite thin layer at a height of 400 km.

In order to assess the obtained results, at first the comparison between the localized ionospheric model and the global ionospheric model – a series of spherical harmonics adapting a single-layer model in a sun-fixed reference frame (Schaer 1997) − was made. The statistics of the comparison have been shown in Table 1 over a typical day and the day number 1 for year 2000 (a year of maximum solar activity), year 2003 (a year of moderate solar activity), and year 2006 (a year of minimum solar activity). Figure 3 illustrates the *Kp* index for the mentioned year. This table shows the differences between the VTEC obtained from the global spherical harmonic coefficients and that from the ground-based GPS observations. Also, it reveals the discrepancy between the VTEC obtained from the localized coefficients and

that from the ground-based GPS observation. The results obtained from the latter are much less than those from the former, indicating the high capability for the proposed method.

Table 1

The statistics on the $VTEC_{GIM} - VTEC_{obs}$ and $VTEC_{localized} - VTEC_{obs}$

Method	GIM		Slepian (localized)	
Epoch	Mean	Standard	Mean	Standard
2000, DOY 1	4.2823	0.7784	1.6897	0.8793
2003, DOY 1	5.7540	0.8686	0.9820	0.9614
2006, DOY 1	3.1916	0.5326	0.6855	0.6241
2013, DOY 1, at 08:00	3.9498	0.5555	1.6373	0.6567
2013, DOY 1, at 12:00	2.2799	0.8920	1.2749	0.6765
2013, DOY 1, at 16:00	4.8667	0.7513	0.9693	0.4579
2013, DOY 1, at 20:00	4.3408	0.7881	1.1186	0.3674

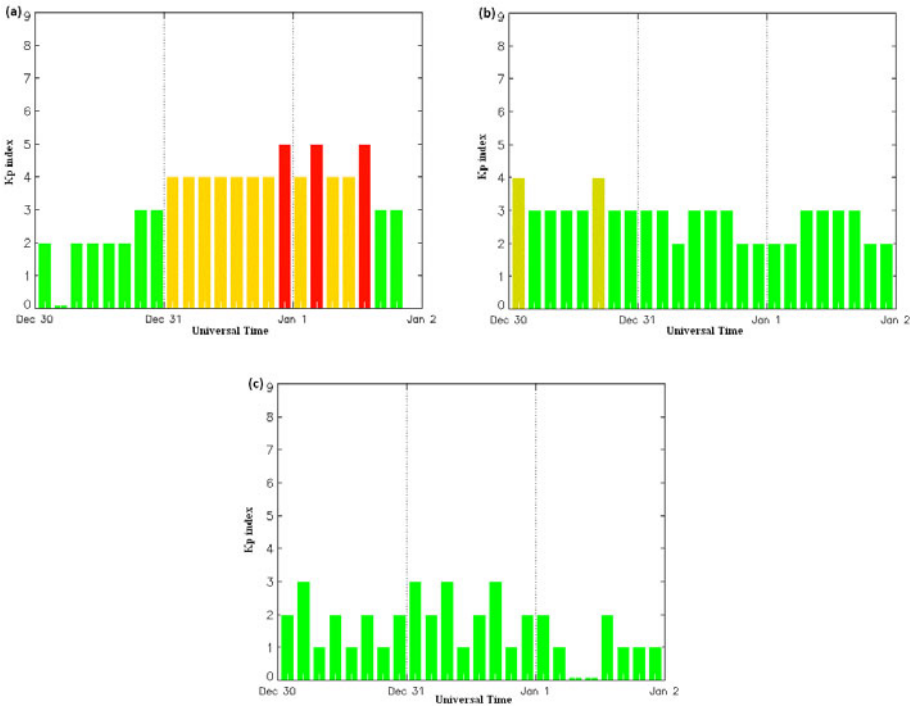

Fig. 3. Estimated planetary *K* index for: (a) Year 2000 Day Number 1, (b) Year 2003 Day Number 1, and (c) Year 2006 Day Number 1 (http://www.spaceweatherlive.com).

Then the comparison between the modeling using the terrestrial GPS and the combined model was made. In other words, at the first step, the Slepian coefficients were obtained using only the ground-based GPS observations and at the next step, these coefficients were combined with the localized coefficients (Eq. 17) utilizing the weighted least-squares method.

For this purpose, the VTEC 2-D modeling was done as a function of the geomagnetic latitude β and the sun-fixed longitude s for a specified time interval $[t_{\min}, t_{\max}]$ (Schaer *et al*. 1995, Wielgosz *et al*. 2003, Sharifi and Farzaneh 2014):

$$\mathrm{TEC}(\beta,s)=\sum_{l=0}^{L}\sum_{m=-l}^{l}\omega_{lm}Y_{lm}(\beta,s)=\sum_{n=l}^{(L+1)^2}\omega_n g_n(\beta,s)\approx\sum_{n=1}^{N}\omega_n g_n(\beta,s)\ , \qquad (19)$$

where $Y_{lm}(\beta,s)$, $g_n(\beta,s)$, and ω are the spherical harmonic, spherical Slepian function, and unknown coefficient, respectively.

The 2-D analyses were conducted assuming that the ionosphere is static for the modeling period by neglecting the relatively small temporal variations in the ionosphere as a function of the geomagnetic latitude β calculated by:

$$\sin\beta=\sin\varphi_g\sin\varphi_0+\cos\varphi_g\cos\varphi_0\cos\left(\lambda_g-\lambda_0\right)\ , \qquad (20)$$

where φ_0 and λ_0 are the geographical coordinates of the geomagnetic pole, φ_g and λ_g are the geographical longitude and latitude of default point. The sun-fixed longitude s can be defined as (Schaer *et al*. 1995, Wielgosz *et al*. 2003):

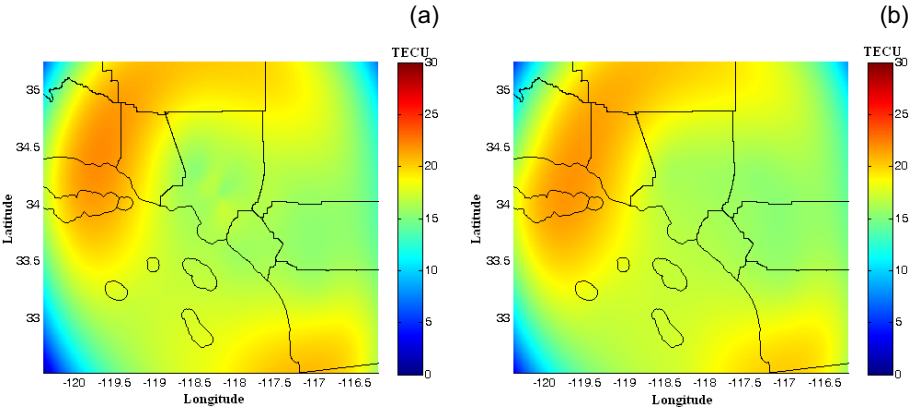

Fig. 4: (a) 2-D VTEC model for 1 January 2013, 01:00:00 UT RMSE = 0.745 TECU; and (b) combined VTEC model for 1 January 2013, 01:00:00 UT RMSE = 0.521 TECU.

$$s = \lambda_g + \mathrm{UT} - \pi = \lambda_g + \left(\mathrm{UT} - 12\right)^{\mathrm{hours}} \quad , \tag{21}$$

where s is in degree and UT is the universal time in hour. The root-mean-square-error (RMSE) value for the residuals is 0.745 Total Electron Content Units (TECU) for 1 January 2013 from t = 00:00:00 UT to t = 02:00:00 UT. Finally, the converted spherical harmonics were updated by the terrestrial GPS observations for the same period. In this case, the RMSE is 0.521 TECU. The VTEC map of the 2-D modeling for the mid-point of the modeling period (01:00:00 UT) and the combined model have been plotted in Fig. 4. The results indicate that by the use of the Slepian functions, an improvement was made.

6. SUMMARY AND CONCLUSIONS

The knowledge of the ionospheric electron density and its variation is essential for a wide range of applications, such as radio telecommunications, satellite tracking, earth observation from space, and satellite navigation. In this study, a spatiospectral localization analysis was conducted utilizing the Slepian basis functions and by use of their properties, the spherical-harmonic coefficients of the GIM were converted into equivalent Slepian coefficients. The results show that the method is novel and efficient in representing and analyzing the regional signals. Besides this, the Slepian coefficients derived from the terrestrial GPS observations were combined with the localized spherical harmonic with the help of the least-squares adjustment, indicating that the combined model is suitable for the regional VTEC modeling rather than the 2-D Slepian modeling.

References

Alizadeh, M.M., H. Schuh, S. Todorova, and M. Schmidt (2011), Global ionosphere maps of VTEC from GNSS, satellite altimetry, and Formosat-3/COSMIC data, *J. Geodesy* **85**, 12, 975-987, DOI: 10.1007/s00190-011-0449-z.

Angrisano, A., S. Gaglione, C. Gioia, M. Massaro, and S. Troisi (2013), Benefit of the NeQuick Galileo version in GNSS single-point positioning, *Int. J. Nav. Observ*. **2013**, 302947, DOI: 10.1155/2013/302947.

Beggan, C.D., J. Saarimäki, K.A. Whaler, and F.J. Simons (2013), Spectral and spatial decomposition of lithospheric magnetic field models using spherical Slepian functions, *Geophys. J. Int.* **193**, 1, 136-148, DOI: 10.1093/gji/ggs122.

Bilitza, D., L.-A. McKinnell, B. Reinisch, and T. Fuller-Rowell (2011), The international reference ionosphere today and in the future, *J. Geodesy* **85**, 12, 909-920, DOI: 10.1007/s00190-010-0427-x.

Ciraolo, L., F. Azpilicueta, C. Brunini, A. Meza, and S.M. Radicella (2007), Calibration errors on experimental slant total electron content (TEC) determined with GPS, *J. Geodesy* **81**, 2, 111-120, DOI: 10.1007/s00190-006-0093-1.

Coster, A.J., E.M. Gaposchkin, and L.E. Thornton (1992), Real-time ionospheric monitoring system using GPS, *Navigation* **39**, 2, 191-204, DOI: 10.1002/j.2161-4296.1992.tb01874.x.

El-Arini, M.B., P.A. O'Donnell, P.M. Kellam, J.A. Klobachar, T.C. Wisser, and P.H. Doherty (1993), The FAA Wide Area Differential GPS (WADGPS) static ionospheric experiment. **In:** *Proc. National Technical Meeting, Institute of Navigation, 20-22 January 1993, San Francisco, USA*, 485-496.

El-Arini, M.B., C.J. Hegarty, J.P. Fernow, and J.A. Klobuchar (1994a), Development of an error budget for a GPS Wide-Area Augmentation System (WAAS). **In:** *Proc. National Technical Meeting, Institute of Navigation, 24-26 January 1994, San Diego, USA*, 927-936.

El-Arini, M.B., R.S. Conker, T.W. Albertson, J.K. Reagan, J.A. Klobuchar, and P.H. Doherty (1994b), Comparison of real-time ionospheric algorithms for a GPS Wide-Area Augmentation System (WAAS), *Navigation* **41**, 4, 393-414, DOI: 10.1002/j.2161-4296.1994.tb01887.x.

Gao, Y., P. Heroux, and J. Kouba (1994), Estimation of GPS receiver and satellite L1/L2 signal delay biases using data from CACS. **In:** *Proc. KIS-94, 30 August – 2 September 1994, Banff, Canada*, 109-117.

García-Fernández, M. (2004), Contributions to the 3D ionospheric sounding with GPS data, Ph.D. Thesis, Technical University of Catalonia, Barcelonna, Spain.

García-Fernández, M., M. Hernández-Pajares, J.M. Juan, J. Sanz, R. Orús, P. Coisson, B. Nava, and S.M. Radicella (2003), Combining ionosonde with ground GPS data for electron density estimation, *J. Atmos. Sol.-Terr. Phys.* **65**, 6, 683-691, DOI: 10.1016/S1364-6826(03)00085-3.

Horn, R.A., and C.R. Johnson (1991), *Topics in Matrix Analysis*, Cambridge University Press, Cambridge.

Komjathy, A. (1997), Global ionospheric total electron content mapping using the Global Positioning System, Ph.D. Thesis, Department of Geodesy and Geomatics Engineering, University of New Brunswick, Fredericton, Canada.

Liao, X., and Y. Gao (2001), High-precision ionospheric TEC recovery using a regional-area GPS network, *Navigation* **48**, 2, 101-111, DOI: 10.1002/j.2161-4296.2001.tb00232.x.

Liu, J., Z. Wang, H. Zhang, and W. Zhu (2008), Comparison and consistency research of regional ionospheric TEC models based on GPS measurements, *Geomat. Inf. Sci. Wuhan Univ.* **33**, 5, 479-483.

Liu, J., R. Chen, H. Kuusniemi, Z. Wang, H. Zhang, and J. Yang (2010), A preliminary study on mapping the regional ionospheric TEC using a spherical cap

harmonic model in high latitudes and the Arctic Region, *J. Glob. Pos. Syst*. **9**, 1, 22-32, DOI: 10.5081/jgps.9.1.22.

Liu, J., R. Chen, Z. Wang, and H. Zhang (2011), Spherical cap harmonic model for mapping and predicting regional TEC, *GPS Solut*. **15**, 2, 109-119, DOI: 10.1007/s10291-010-0174-8.

Liu, J., R. Chen, J. An, Z. Wang, and J. Hyyppa (2014), Spherical cap harmonic analysis of the Arctic ionospheric TEC for one solar cycle, *J. Geophys. Res.* **119**, 1, 601-619, DOI: 10.1002/2013JA019501.

Mautz, R., J. Ping, K. Heki, B. Schaffrin, C. Shum, and L. Potts (2005), Efficient spatial and temporal representations of global ionosphere maps over Japan using B-spline wavelets, *J. Geodesy* **78**, 11-12, 660-667, DOI: 10.1007/s00190-004-0432-z.

Mikhail, E.M., and F.E. Ackermann (1976), *Observations and Least Squares*, IEP Series in Civil Engineering, Dun-Donnelley, New York, 497 pp.

Nohutcu, M., M.O. Karslioglu, and M. Schmidt (2010), B-spline modeling of VTEC over Turkey using GPS observations, *J. Atmos. Sol.-Terr. Phys*. **72**, 7-8, 617-624, DOI: 10.1016/j.jastp.2010.02.022.

Percival, D.B., and A.T. Walden (1993*), Spectral Analysis for Physical Applications: Multitaper and Conventional Univariate Techniques*, Cambridge Univ. Press, Cambridge.

Radicella, S.M., B. Nava, and P. Coïsson (2008), Ionospheric models for GNSS single frequency range delay corrections, *Fís. Tierra* **20**, 27-39.

Schaer, S. (1997), How to use CODE's Global Ionosphere Maps, Astronomical Institute, University of Berne, Switzerland, http://www.aiub.unibe.ch.

Schaer, S. (1999), Mapping and predicting the Earth's ionosphere using the Global Positioning System, Ph.D. Thesis, Astronomical Institute, University of Berne, Switzerland.

Schaer, S., G. Beutler, L. Mervart, M. Rothacher, and U. Wild (1995), Global and regional ionosphere models using the GPS double difference phase observable. **In:** G. Gendt and G. Dick (eds.), *Proc. IGS Workshop on Special Topics and New Directions, 15-18 May 1995, GFZ, Potsdam, Germany*, 77-92.

Schaer, S., G. Beutler, M. Rothacher, and T.A. Springer (1996), Daily global ionosphere maps based on GPS carrier phase data routinely produced by the CODE analysis center. **In:** R.E. Neilan *et al*. (eds.), *Proc. IGS Analysis Center Workshop, Silver Spring, USA, 19-21 March 1996*, 181-192.

Schmidt, M. (2007), Wavelet modelling in support of IRI, *Adv. Space Res*. **39**, 5, 932-940, DOI: 10.1016/j.asr.2006.09.030.

Schmidt, M., D. Bilitza, C.K. Shum, and C. Zeilhofer (2008), Regional 4-D modeling of the ionospheric electron density, *Adv. Space Res.* **42**, 4, 782-790, DOI: 10.1016/j.asr.2007.02.050.

Schunk, R.W., L. Scherliess, J.J. Sojka, D.C. Thompson, D.N. Anderson, M. Codrescu, C. Minter, T.J. Fuller-Rowell, R.A. Heelis, M. Hairston, and

B.M. Howe (2004), Global Assimilation of Ionospheric Measurements (GAIM), *Radio Sci.* **39**, RS1S02, DOI: 10.1029/2002RS002794.

Sharifi, M.A., and S. Farzaneh (2014), The spatio-spectral localization approach to modelling VTEC over the western part of the USA using GPS observations, *Adv. Space Res*. **54**, 6, 908-916, DOI: 10.1016/j.asr.2014.05.005.

Simons, F.J. (2010), Slepian functions and their use in signal estimation and spectral analysis. **In:** W. Freeden, M.Z. Nashed, and T. Sonar (eds.), *Handbook of Geomathematics*, Springer, Berlin Heidelberg, 891-923, DOI: 10.1007/978-3-642-01546-5_30.

Simons, F.J., F.A. Dahlen, and M.A. Wieczorek (2006), Spatiospectral concentration on a sphere, *SIAM Rev*. **48**, 3, 504-536, DOI: 10.1137/S0036144504445765.

Simons, M., S.C. Solomon, and B.H. Hager (1997), Localization of gravity and topography: constraints on the tectonics and mantle dynamics of Venus, *Geophys. J. Int.* **131**, 1, 24-44, DOI: 10.1111/j.1365-246X.1997.tb00593.x.

Skone, S.H. (1998), Wide area ionosphere grid modelling in the auroral region, Ph.D. Thesis, UCGE Report No. 20123, University of Calgary, Calgary, Canada.

Slepian, D. (1983), Some comments on Fourier analysis, uncertainty and modeling, *SIAM Rev*. **25**, 3, 379-393, DOI: 10.1137/1025078.

Stolle, C., S. Schlüter, Ch. Jacobi, and N. Jakowski (2003), 3-dimensional ionospheric electron density reconstruction based on GPS measurements, *Adv. Space Res.* **31**, 8, 1965-1970, DOI: 10.1016/S0273-1177(03)00168-6.

Tegmark, M. (1997), How to measure CMB power spectra without losing information, *Phys. Rev. D* **55**, 10, 5895-5907, DOI: 10.1103/PhysRevD.55.5895.

Wieczorek, M.A., and F.J. Simons (2005), Localized spectral analysis on the sphere, *Geophys. J. Int*. **162**, 3, 655-675, DOI: 10.1111/j.1365-246X.2005.02687.x.

Wielgosz, P., D. Grejner-Brzezinska, and I. Kashani (2003), Regional ionosphere mapping with kriging and multiquadratic methods, *J. GPS* **2**, 1, 48-55, DOI: 10.5081/jgps.2.1.48.

Wu, Y., S.G. Jin, Z.M. Wang, and J.B. Liu (2010), Cycle slip detection using multi-frequency GPS carrier phase observations: A simulation study, *Adv. Space Res*. **46**, 2, 144-149, DOI: 10.1016/j.asr.2009.11.007.

Zeilhofer, C. (2008), Multi-dimensional B-spline modeling of spatio-temporal ionospheric signals, Deutsche Geodätische Kommission, Bayerischen Akademie der Wissenschaften, München, Germany.

Received 5 August 2014
Received in revised form 23 December 2014
Accepted 15 January 2015